

DARPA
Instant Flame Suppression
Phase II - Final Report

Harvard: Acoustic Suppression

- 1. Introduction**
- 2. Flame Extinction by Transverse Acoustic Waves**
 - 2.1. Summary**
 - 2.2. Experimental Details**
 - 2.3. Results**
 - 2.3.1. Burner Material**
 - 2.3.2. Fuel Velocity**
 - 2.3.3. Reynolds Number**
 - 2.4. Discussion**
- 3. Acoustic Cavities**
 - 3.1. Summary**
 - 3.2. Numerical Modeling**
 - 3.3. Experimental Results**
- 4. Mechanism and Theory**
 - 4.1. Summary**
 - 4.2. Basic Mechanism**
- 5. Scale-up: Limitations and Opportunities**
 - 5.1. Limitations**
 - 5.2. Opportunities**
- 6. References**

Appendix 1. P-P Method

Appendix 2. Total Air Displacement from Measured Velocities

1. Introduction

We investigated the interactions of acoustics waves with flames, in a parallel study to electric and electromagnetic interactions. The interaction between sound and flames was first reported by John Leconte in 1858, who noted that flames within an orchestral hall respond to beats within music. The phenomenon of sound interacting with flames would be used in the study of combustion instabilities and feedback controls¹⁻³, instabilities within rocket propulsion^{4,5}, turbine combustion⁶⁻⁸, flame manipulation^{9,10}, enhancement¹¹, and extinction¹²⁻¹⁸. Key to the mechanoacoustic manipulation of flames is the work of W.R. Babcock, who in 1967, reported the use of flames as an acoustic amplifier¹⁹. In this work, the flame surface was modulated by induced instabilities (either within the feed gas, or through an applied electric field), resulting in sound being emitted from the surface of the flame. This paper was the first experimental report describing the surface tension of a flame.

Previous work on acoustic interactions with flames has covered a range of systems, including pre-mixed flames²⁰, droplets^{5,21}, and acoustic forcing of diffusion flames^{11,22,23}. In these studies, the most commonly proposed mechanisms for the coupling of acoustics with flames included 1) periodic oscillation of the equivalence ratio (air-fuel ratio)^{24,25}, 2) oscillations of the total flame induced by convective forces²⁶, 3) oscillations of the flame area induced by acoustic accelerations²⁷⁻²⁹, 4) sensitivity of the chemical reaction rate of the flame to local pressure^{30,31}. Phase I studies of mechanoacoustic manipulation of flames investigated the previously uncharacterized phenomenon of acoustic extinction of a diffusion flame by coupling with a transverse acoustic source. These studies investigated the relationship between flame extinction and the applied acoustic frequency, velocity, and pressures. Ultimately, we found that the local air velocity imparted at the flame body is the dominant factor in the extinction of the studied flames. Phase II studies investigated the extinction of liquid pool flames, as well as investigated the scale up potential of acoustic extinction methods.

2. Flame Extinction by Transverse Acoustic Waves

2.1. Summary. During Phase I, we investigated the extinction of a 15-cm non-premixed methane flame exposed to acoustic excitation ranging from 35-150 Hz with pressures ranging from 0.2 Pa (80 dB) to 112 Pa (135 dB). The sound source was a commercial speaker; and we measured its output with a high pressure decibel meter. Although the initial study described a frequency dependence of flame suppression (peak extinctions were observed near 60 Hz) when measuring acoustic pressures, we later deduced that the observed peak in pressure at 60 Hz did not correspond to a peak in acoustic velocity at the location of the excited flame. Subsequent experiments would measure acoustic velocities of the air surrounding the flame, simultaneously with the acoustic frequency and pressure. We found that a threshold acoustic velocity must be applied to the flame in order to achieve extinction, rather than a specific frequency or acoustic pressure. The threshold extinction velocity (acoustic velocity at which extinction occurs) is also a function of the stability of the flame. In the case of gaseous fuel sources, flame stability is dependent on the flow velocity, and subsequently, the Reynolds number of the exiting fuel stream. One can achieve the threshold extinction velocity, at most frequencies, provided the applied acoustic amplitude (pressure) is sufficient. The air velocity created by the acoustic source was measured using a range of techniques including the p-p method, and MicroflownTM sensors.

2.2. Experimental Details. A schematic of the basic experimental setup is given in **Figure 1A**. This represents the setup used to introduce a single acoustic source to the flame. We modified a commercial subwoofer (QSC model #181i) with a modular collimator constructed of 20ga stainless steel. Without the collimator, the acoustic pattern would exit the speaker in a radial pattern. A burner (connected to a fuel source, commonly methane) was placed in front of the collimator so that the base of the flame was centered with the speaker (**Figure 1B**). Several variables of the burner were investigated including the construction material, fuel velocity, and burner geometry. We placed the sensor (microphones, MicroflowTM, etc.) offset from the burner by 5cm. The Microflow sensor was used to simultaneously measure air velocity and sound pressure, this was also accomplished through the use of a series of microphones utilizing the p-p method (Appendix 1).

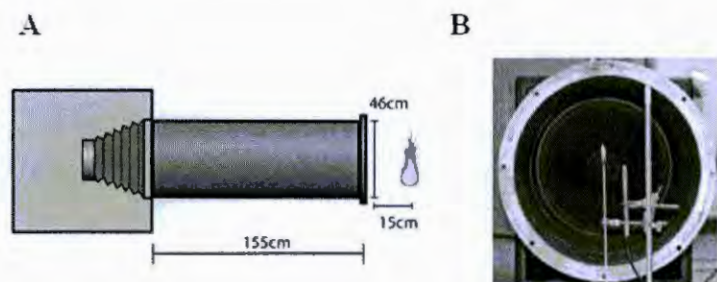


Figure 1. (A) Acoustic setup for extinction of a flame with a subwoofer depicted on the left, a collimator, and a flame on the right. (B) Photo looking into the collimator showing the cone of a subwoofer, a flame, and a Microflow sensor.

The collimator provided an approximately planar wave front to interact with the flame¹⁵. We observed several phenomena with the collimator 1) within the collimator a 6 fold increase in pressure is measured at the speaker face compared to that of a bare speaker, 2) measuring the flame 15 cm in front of the collimator (170cm from the speaker face) has an increase of 144 Pa over the SPL measured 15 cm from the open speaker (**Figure 2**). The majority of the experiments were performed with the flame source 15 cm outside the collimator.

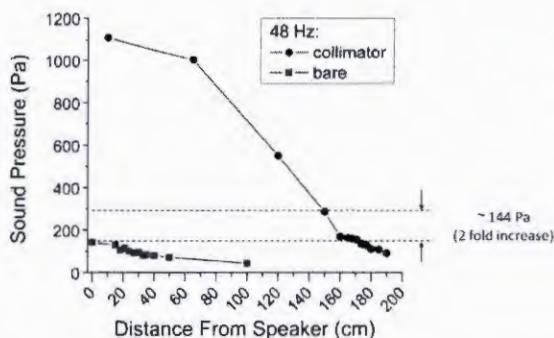


Figure 2. Comparison of measured levels of sound pressure of an open (bare) and collimated speaker. We excited the speaker at 48Hz (with an input voltage of 1Vpp) and measured SPL readings from the face of the speaker.

2.3. Results. Several variables were found to influence the extinction of a non-premixed diffusion flame exposed to transverse acoustic waves. In Phase I, we were limited to measuring pressure and frequency due to available equipment. Using these two parameters, we observed, a frequency dependence with acoustic extinction. The use of 60 Hz was found to be optimal for

extinction events. Similar results had also been reported previously¹². In these studies and our own, the amplitude of the speaker was normalized at the studied frequencies. Due to the output performance of speakers, as well as the test environment, less power was needed to move the air at resonant modes within the room. Thus, when the speaker output was at a lower power setting, we created higher acoustic velocities near resonances of the test chamber which was ~59 Hz. If we increased the output of the speaker, we were able to generate higher air velocities at other frequencies, demonstrating that there was no frequency dependence with acoustic suppression of flames.

Experiments in Phase II investigated the velocity of the air at the flame generated by the acoustic source. **Figure 3** presents an extinction profile of a small methane flame. We present the minimum thresholds to cause ten consecutive extinctions. In these experiments, we measured the dependence of frequency on pressure, velocity, and local displacement near the flame -- measured via the p-p method. In **Figure 3A**, we note that a minimum in the pressure occurred at 60 Hz near one of the resonant modes of the room. A general trend was observed as

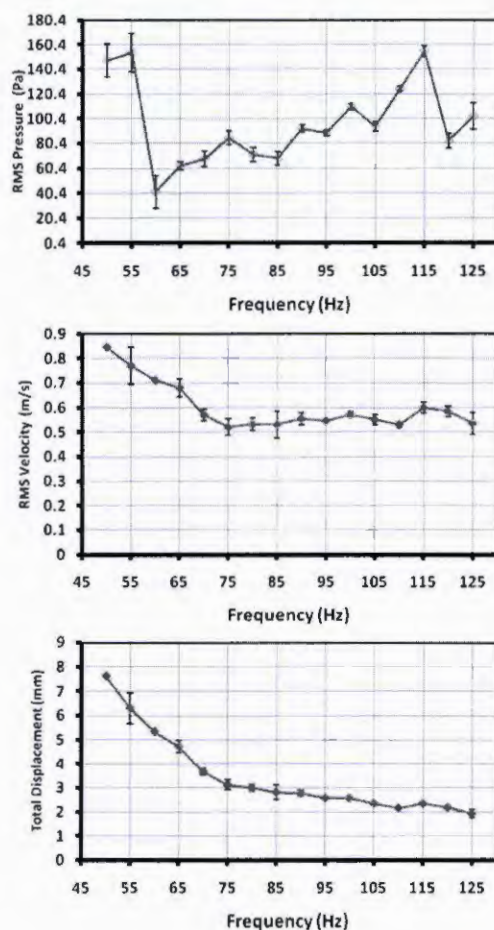


Figure 3. Acoustic extinction profile of a 1.6 mm ID methane burner. Data collected represents acoustic thresholds to create ten consecutive extinction events. Presented are the profiles of pressure (A), velocity (B) and total displacement (C) against frequency. The feed rate of methane to the burner was 100 ml/min.

a higher acoustic pressure was needed to extinguish flames as the frequency increased.

Figure 3B displays a decrease in air velocity as frequency increased; however, there is a minimum velocity observed to extinguish the flame ($\sim 0.5\text{m/s}$). Lastly, we calculated the air displacement for the system (**Figure 3C**). The derivation of these values is found in Appendix 2.

2.3.1. Burner Material. We found that the burner material had no significant impact on the extinction event. In **Figure 4**, we display the extinction profiles of acoustic pressure (top) and velocity (bottom) for burners with the same fuel source (methane), burner diameter (ID = 0.0625") and fuel flow rate (200 sccm). We surveyed frequencies from 50-130 Hz, measuring the extinction threshold for these burners; increasing the amplitude of the speaker until ten consecutive extinctions occurred. The data represents the average velocity and pressures during the ten consecutive extinction events.

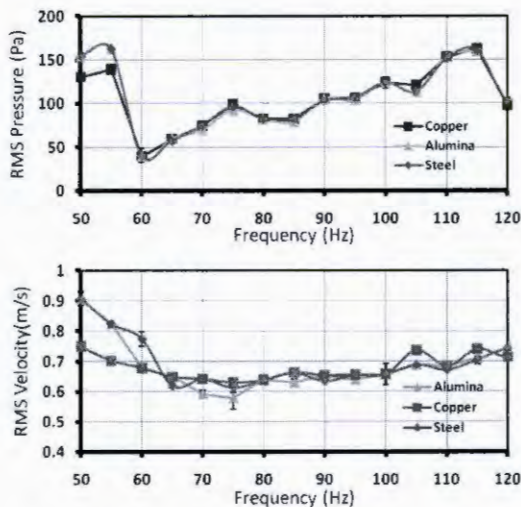


Figure 4. Dependence of flame extinction on burner material. We measured the threshold extinction pressure (top) and velocity (bottom) of methane burners made from alumina ceramic, copper, and stainless steel with a constant ID of 0.125" and a flow rate of 200sccm.

2.3.2. Fuel velocity. In **Figure 5**, we display the threshold extinction properties of a 75 Hz acoustic source as the fuel velocity to the burner was increased. We changed the fuel velocity of a non-premixed methane burner and measured the acoustic pressure (not shown) and velocities necessary to create ten consecutive extinctions. The flame underwent a transition from laminar to turbulent at a flow rate of 18.1 m/s, where the Reynolds number was approximately 2000. The fuel velocity was increased until conditions caused a lifted flame (occurring above 24.5 m/s; $Re = 2700$) in the system. We did not measure the acoustic extinction of a lifted flame.

Within laminar conditions, the acoustic velocity necessary to extinguish the flame increased with the fuel velocity with a plateau at $\sim 1.45\text{ m/s}$ for acoustic velocity. As the fuel velocity increased past 18.1 m/s, the flame becomes turbulent, and the acoustic velocity necessary for extinction decreased rapidly. This trend was observed at multiple acoustic frequencies, supporting the hypothesis that acoustic velocity contributed to the extinction of the flame and that extinction was also dependant on the stability of the flame.

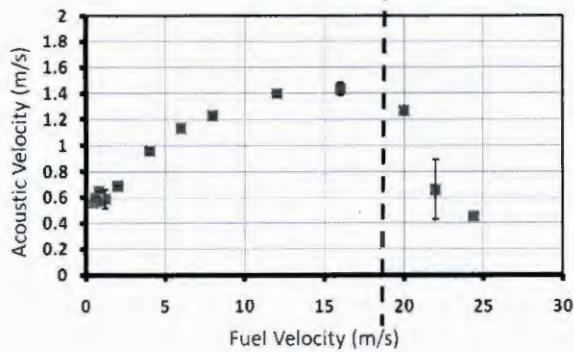


Figure 5. Dependence of flame extinction on fuel velocity. Threshold extinction of a methane flame exposed to a 75 Hz acoustic source. Turbulence is exhibited in the flame at fuel velocities above 18 m/s. The flame was generated using a 0.0625" ID ceramic burner.

2.3.3. Reynolds Number. One can further compare the effect of the Reynolds number of the fuel on flame extinction. The calculation of the Reynolds number requires knowledge of the burner geometry and either the flow rate and kinematic viscosity of the fuel or fuel velocity, density, and fluid viscosity. We measured the extinction threshold using ceramic burners with diameters of 0.0625", 0.125", and 0.25". The fuel flow rates were varied so that the Reynolds number for the exiting fuel was 93 in all burners (**Figure 6A**). Details of these conditions are given in Table 1. The averages acoustic velocities for frequencies above 70 Hz were 0.54 m/s (0.0625"), 0.65 m/s (0.125") and 0.77 m/s (0.25"). The acoustic velocities are of the same magnitude as the velocity of the fuel exiting the burner.

Using the same burners, we varied the fuel delivery such that the fuel exited at 1.0 m/s (**Figure 6B**). The Reynolds for these burners were 110 (0.0625"), 220 (0.125"), and 440(0.25"). As the Reynolds value for the burner increased, the acoustic velocity necessary for extinction increased. We also note that the required acoustic velocity for extinction increased with frequency in these experiments.

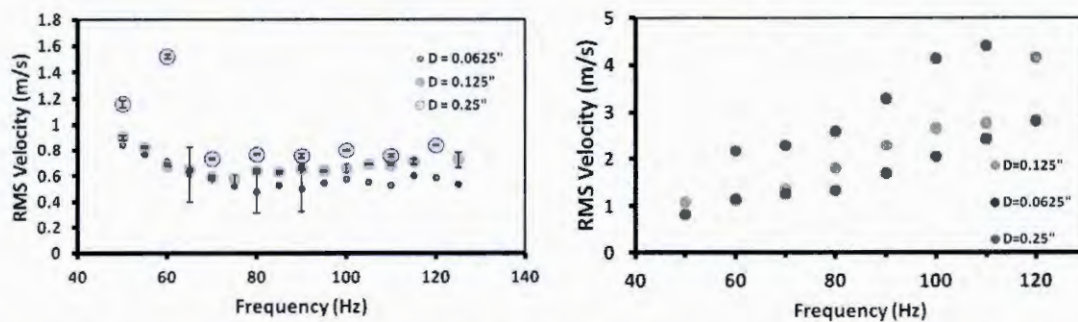


Figure 6. Dependence of RMS acoustic velocity on frequency. The response of ceramic burners with varying internal diameters (0.0625", 0.125", and 0.25") was measured. Fuel flow rates were adjusted to have constant Reynolds number (A), and constant fuel velocity (B).

Table 1

Burner Diameter	Flow Rate (sccm)	Fuel Velocity (m/s)	Re	Avg. Acoustic Extinction Velocity (m/s)
0.0625"	100	0.84	93	0.54
0.125"	200	0.42	93	0.68
0.25"	400	0.21	93	0.77

2.4. Discussion. We have demonstrated that acoustic suppression of flames does not occur at a specific frequency nor pressure, rather it is strongly dependant on the local air displacement at the body of the flame. The nature of acoustics is such that the air velocity of a sound wave is a convolution of the wave frequency and pressure, thus there is an indirect dependence on these variables. One can generate a specific air velocity using various combinations of pressure and frequency. In our studies, we had precise control over these acoustics and were able to measure the conditions and thresholds for extinction. These are very ideal conditions; in a real fire, one would not have *a priori* knowledge about the source of a flame (fuel rate, burner area, etc.). By exposing a random flame to a sound source that modulates frequency and pressure, we would expose the flame to various air velocities that might lead to extinction, provided the applied acoustic velocity were greater than the extinction threshold for a duration long enough to cause extinction.

3. Acoustic Cavities

3.1. Summary. Extinction in a room generally requires localized mobilization of instruments and delivery of material to address a fire. By coupling to the resonant modes of an acoustic cavity, there is the potential to extinguish flames at-a-distance or at specified locations such as anti-nodes within a room. To explore extinction of flames in acoustic cavities, we ran simulations for acoustic fields with different geometries (initial guidance provided by Doug Ladouceur and Jim Fleming at the Navy Research Labs) and experiments on Harvard's campus and at Hanscom Air Force Base.

To model the acoustics in a cavity, we started with two-dimensional models as shown in **Figure 7**. While we do not include the magnitude for the simulated results, these plots show standing waves of pressure and velocity in a cavity and their dependence on the frequency/wavelength of excitation (excited region was at the internal, vertical edge of the cup-like collimator).

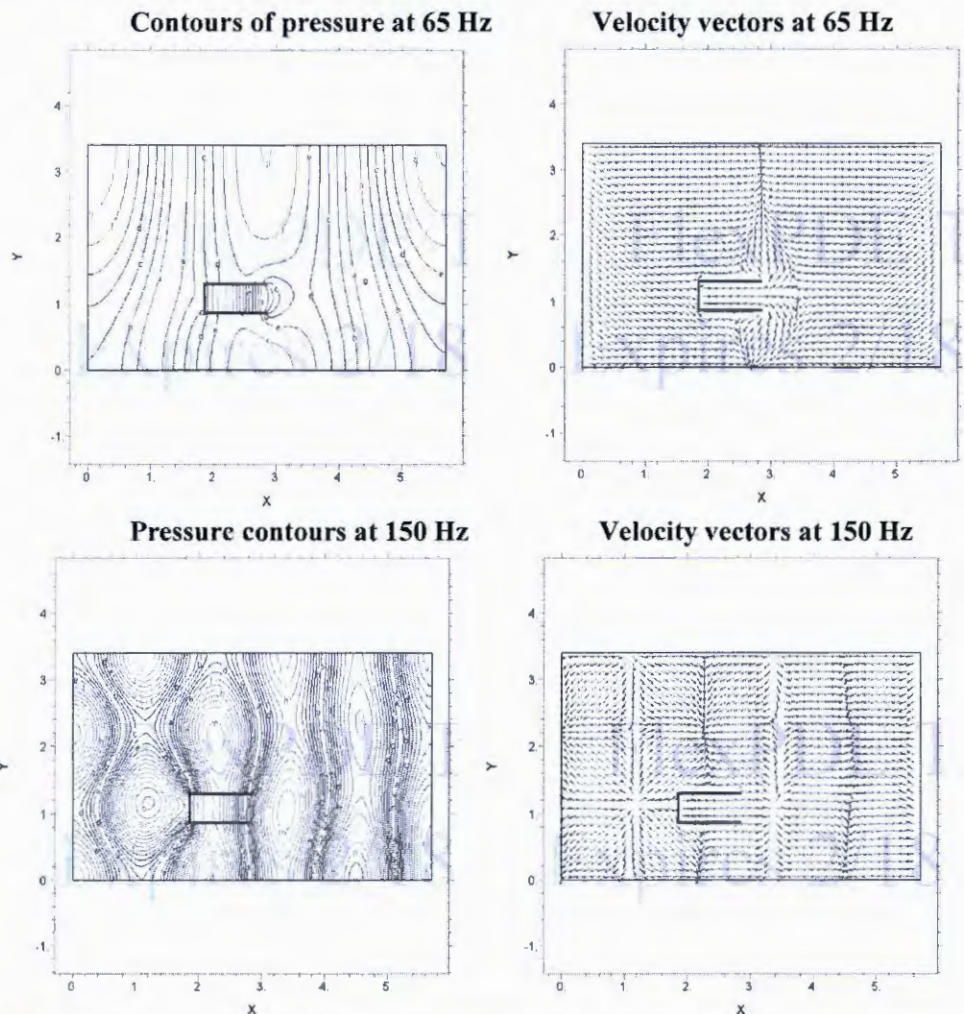


Figure 7. 2-D acoustic simulations for pressure and velocity in a box with a collimator. The inner vertical wall of the collimator is excited. The height of the box is 3.4 m, while the length/width of the box is 3.7 m.

3.2. Numerical Modeling. We used the software package FlexPDE to model the acoustic fields with different geometries. The partial differential equation governing the physics came from standard derivations neglecting viscosity (an e-book from Backstrom <http://ebooks.ebookmall.com/ebook/411296-ebook.htm> and Landau and Lifshitz's **Fluid Mechanics** p. 251).

$$\frac{\partial \rho}{\partial t} + \rho \nabla \cdot \vec{v} = 0 \quad \text{Continuity}$$

$$\frac{\partial \vec{v}}{\partial t} + \frac{\nabla p}{\rho} = 0 \quad \text{Euler's equation (small velocities)}$$

Set $\vec{v} = -\nabla \phi$ and $\phi = (\phi_r + j\phi_i)e^{j\omega t}$

$$\nabla^2 \phi + \frac{\rho \omega^2}{B_s} \phi = 0$$

$$p = \rho \frac{\partial \phi}{\partial t}$$

The boundary conditions for reflective walls were $\hat{n} \cdot \nabla \phi_r = 0$ and $\hat{n} \cdot \nabla \phi_i = 0$, while the boundary conditions for oscillating/vibrating walls were $\hat{n} \cdot \nabla \phi_r = \text{amplitude of velocity}$ and $\hat{n} \cdot \nabla \phi_i = 0$. To calculate velocities and pressures, we solved for ϕ to find $\vec{v} = \vec{v}_r \cos(\omega t)$ and $p = -p_i \sin(\omega t)$. **Figure 8** shows a 3-D geometry and configuration of a mesh created in FlexPDE. With the boundary condition on all surfaces except for the excited surface set to be reflective ($\hat{n} \cdot \nabla \phi_r = 0$ and $\hat{n} \cdot \nabla \phi_i = 0$), and the excited surface (internal, vertical disc within the cup-like collimator) set to have a velocity of 1 m/s ($\hat{n} \cdot \nabla \phi_r = \text{amplitude of velocity}$ or 1 m/s and $\hat{n} \cdot \nabla \phi_i = 0$), **Figure 9** shows sliced contours depicting the acoustic pressures and velocities in the chamber.

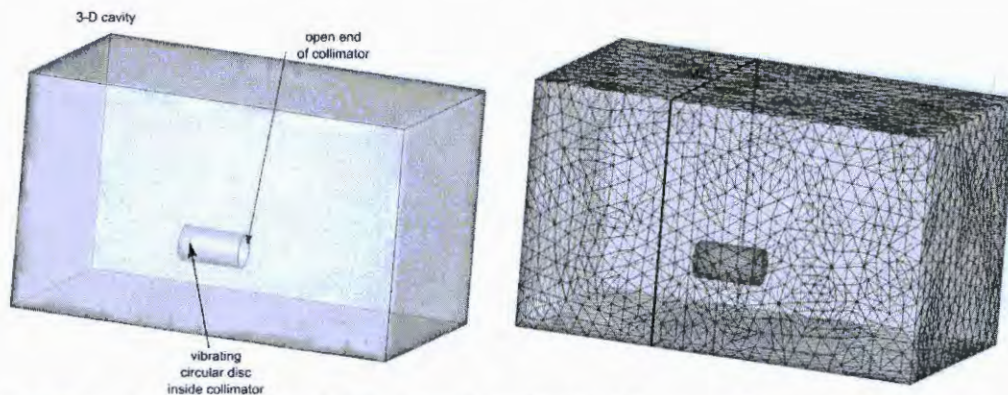


Figure 8. Geometry for modeling acoustic excitation of a room. Dimensions of the box are 3.4 m x 3.4 m x 5.7 m.

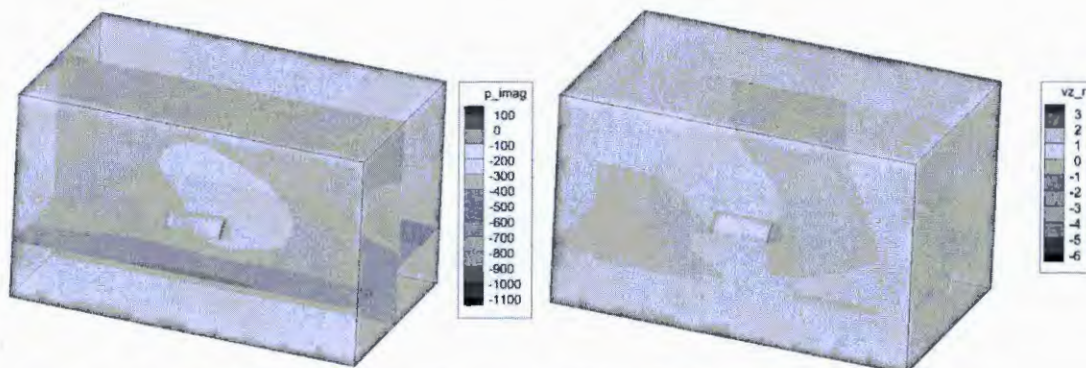


Figure 9. Simulated results for acoustic pressure (Pa) and velocity (m/s) at 100 Hz.

Experimental Results. Without excitation of a flame, we compared experimental measurements of acoustic pressures and velocities within the room in the basement of our building in which we normally performed experiments. **Figure 10** provides a side-by-side comparison between normalized experimental data and the simulated results at specified locations within the room. Even without including the viscosity term in our acoustic modeling of the room and assuming the walls to be lossless in their reflection of acoustic waves, there is reasonable agreement between the experimental data and the simulations over the ranges of frequency of interest for acoustic extinction of flames. **Figure 11** shows the characterization of the acoustic velocities at the circled location shown in **Figure 10** as a function of the frequency of excitation. The general hypothesis was that for the methane-based diffusion flames, peaks in acoustic velocities would be effective for extinguishing flames.

Extinction was possible at different locations within the room we used in the basement of our building at Harvard. The approximate dimensions of the room were 5.7 m (length) x 3.3 m (width) x 3.2 m (height). In one case, we were able to extinguish flames with a frequency of 60 Hz at a distance of 1.06 m to the left of the center axis of the collimator and 1.64 m in front of the collimator. The initial experiments with extinction of flames away from the collimator used unstable, turbulent flames. While impressive in appearance, these flames were very sensitive to changes in the flow rate of methane and surrounding convective flows. We performed additional experiments in the same room at Harvard using a “mini-flame” shown in **Figure 12**. **Figure 13** shows that we were able to extinguish the mini-flame at the expected frequencies of 60 Hz and 80 Hz, but we also had extinction at 50 Hz and lack a good explanation for this behavior.

On June 22, Albert Viggiano hosted us as we performed experiments in two rooms at Hanscom Airforce Base. Todd Pedersen also helped us make arrangements for tests. Prior to running tests at Hanscom Air Force Base, we had demonstrated efficient extinction at 60 Hz in our room in the basement at Harvard. We had hypothesized the result was due to the tests being conducted in a room with resonance near 60 Hz.

At Hanscom Airforce Base, we tested the hypothesis that the dimensions of a room/acoustic cavity could influence our ability to extinguish flames with acoustic perturbation. We confirmed this hypothesis by being able to extinguish a flame at a mode/frequency (64 Hz) of resonance with a flame 2 m away from the end of the collimator of our system for acoustic excitation, but not at neighboring frequencies (50 Hz, 54 Hz, 60 Hz, and 70 Hz) (**Figure 14**). The length of the room was 5.4 m and had a corresponding mode at 64 Hz (343 m/s divided by 5.4 m = 64 Hz). With extinction of our flame possible at 64 Hz but not 50, 54, 60 and 70 Hz (subwoofer began to clip), our measurements suggest that the spike in velocity is responsible for extinction.

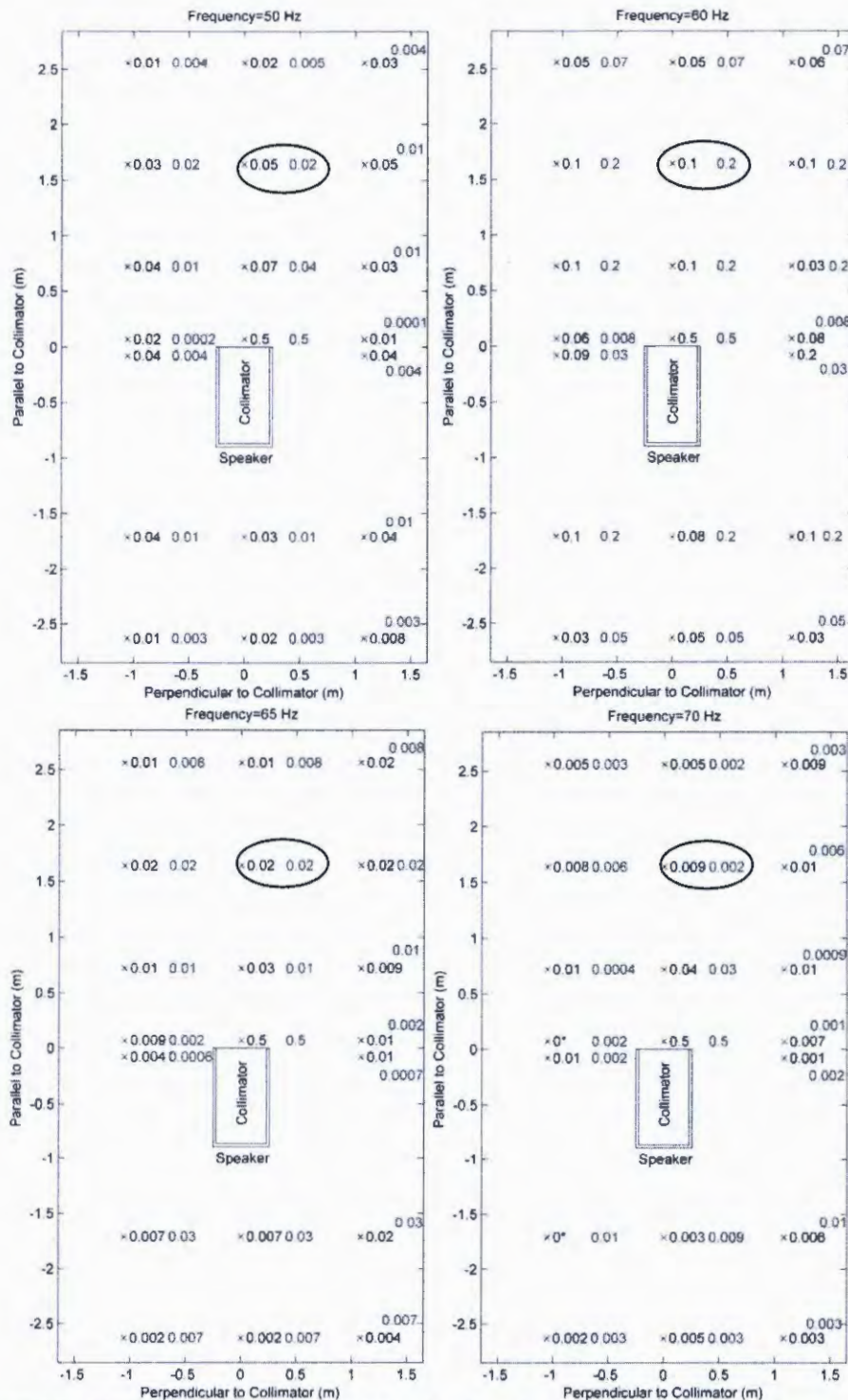


Figure 10. Measured and modeled RMS velocities (m/s) parallel to the collimator in the horizontal plane that bisects the collimator (0.76 m off the ground in the model and 0.43 m off the ground in the actual experiments). The x's show the locations of the measurements, the numbers immediately to the right of the x's show the measured velocity, and the numbers in red (to the right of the measured velocity) show the modeled velocity.

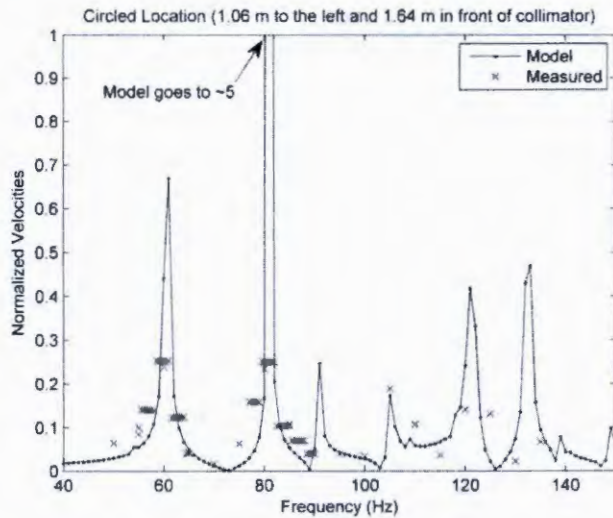


Figure 11. RMS velocity versus frequency at the location circled in Figure 10. The blue dots represent simulated values, and the red x's represent experimentally measured values.

Figure 12. A mini-flame used for characterizing extinction in acoustic cavities. The inner diameter of the ceramic burner was 0.6 mm, and the outer diameter was 0.9 mm. The flow rate of methane through the burner into atmospheric conditions was 23 ml/min with a corresponding vertical velocity of 1.4 m/s for the methane in the tube.

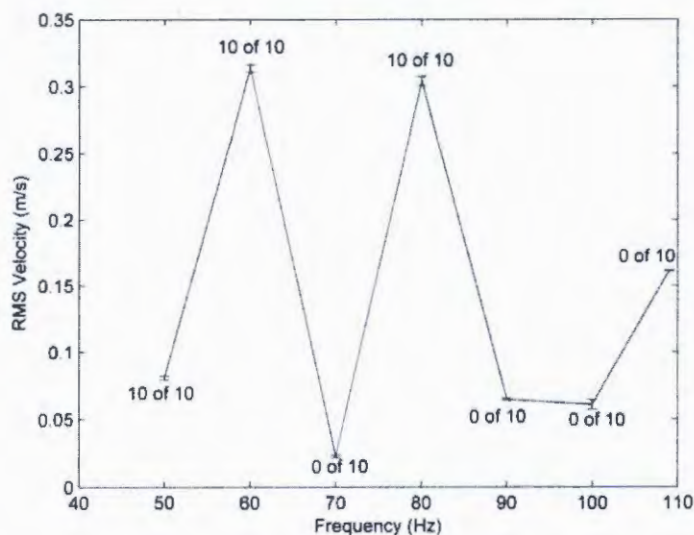


Figure 13. Measured events of excitation of the mini-flame in the room of the basement at Harvard. The flame was at the same circled location shown in Figure 10. At 60 Hz and 80 Hz, excitation of the mini-flame led to extinction 10 out of 10 times as expected based on the measurements and modeling shown in Figure 11. At 70 Hz, 90 Hz, 100 Hz, and 100 Hz, excitation did not led to extinction of the flame. There is not a good explanation currently for the extinction of the mini-flame at 50 Hz.

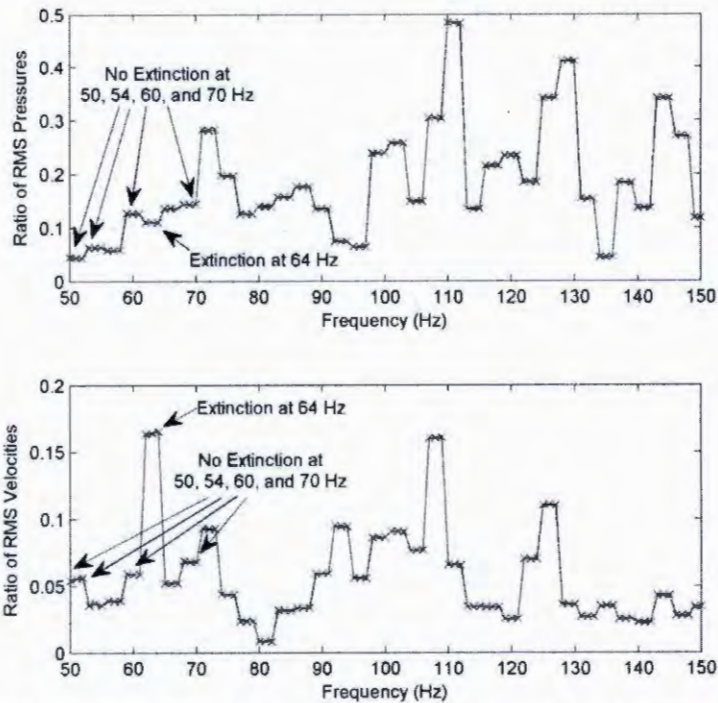


Figure 14. Data collected in a small room (17 ft. 10 in x 13 ft. x 10 ft tall) at Hanscom Airforce Base with normalized pressures and velocities measured at a location of interest. The location of interest was approximately 2 m from the front of the collimator at an angle of 53 degrees relative to the line running through the center of the collimator, and the location of reference was 0.07 m in front of the collimator.

Additionally, we tested the extinction of a flame at the face of a wall. The objective was to decouple the contributions of acoustic pressure and velocity, as velocity would theoretically be zero at the wall. We hypothesized that it would not be possible to extinguish a flame close to a wall of an acoustic cavity since the velocity at a reflecting wall would be zero. We did not fully develop this set of experiments, but initial results demonstrated that the velocity normal to the wall was not necessary to extinguish a flame at that surface. We placed a small flame at different distances from a wall (3, 10, 22, 53 and 83 cm) behind the subwoofer in our room in the basement. **Figure 15** shows the measured acoustic pressures and velocities (normal to the wall) for extinguishing a flame in 10 consecutive attempts at each specified distance from the wall. To illustrate a lower limit of extinction, the red x's show series of 10 consecutive attempts that did not extinguish the flame every time. The results shown suggest that acoustic velocity normal to the wall is not necessary to extinguish a flame. Nevertheless, there might have been velocities parallel to the wall surface that contributed to extinction of the flame.

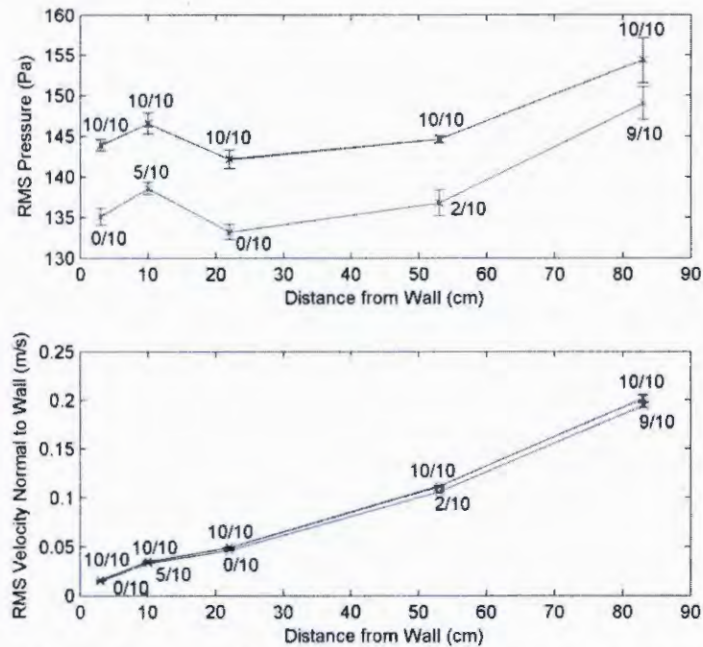


Figure 15. Extinction of a small non-premixed flame of methane (~1 cm in height) placed at different locations from a wall behind a speaker in the basement of our lab. The frequency of excitation was 60 Hz, and the burner had an inner diameter of 0.6 mm and an outer diameter of 0.9 mm. The velocity at the opening of the burner was approximately 3 m/s (based on a flow rate of 50 ml/min). The error bars are $\pm 1 \sigma$.

4. Mechanism and Theory

4.1. Summary. We have demonstrated that oscillations in the local air velocity at the flame body contribute to events of acoustic extinction. We must now consider how a local oscillating air velocity can cause extinction of a flame. Is this analogous to directly blowing air on the flame or do we couple into hydrodynamic forces that influence combustion? We originally presented several possible mechanisms of acoustic coupling with flames 1) periodic oscillation of the air-fuel ratio, 2) oscillations of the flame induced by convective forces, 3) oscillations of the flame area induced by acoustic accelerations and 4) sensitivity of the chemical reaction rate of the flame to local pressure. We have observed some of these mechanisms during our experiments.

4.2. Basic Mechanism. We believe that the primary acoustic mechanism of suppression of gaseous fuels is, in part, a blow-off mechanism; where the acoustic wave imparts kinetic energy to the reactants of the flame causing the net velocity of reactants to be greater than the flame propagation velocity. This conclusion was reached following several experiments with high speed video as well as during studies of flame stability under acoustic excitation (section 2.3.2).

High speed imaging of extinguished flames demonstrated several features of blow-off occurring. In **Figure 16A** a methane flame oscillates about the burner under acoustic excitation. The flame detaches from the burner prior to extinction after approximately 1.7 s. **Figure 16B** displays a flame with a fuel rate of 20 m/s (a turbulent fuel regime). Initially, the total flame underwent oscillations about the burner. Shortly after acoustic excitation, the flame lifted off of the burner but did not extinguish. The flame appeared to undergo chaotic mixing in the lifted

state as it oscillated within the acoustic field; this mixed state represented induced changes in the gradient between fuel and oxidizer. Eventually, the acoustic perturbation extinguished the flame in its lifted state. Since the flame existed in the lifted state, we can conclude that lift-off alone was insufficient to extinguish the flame.

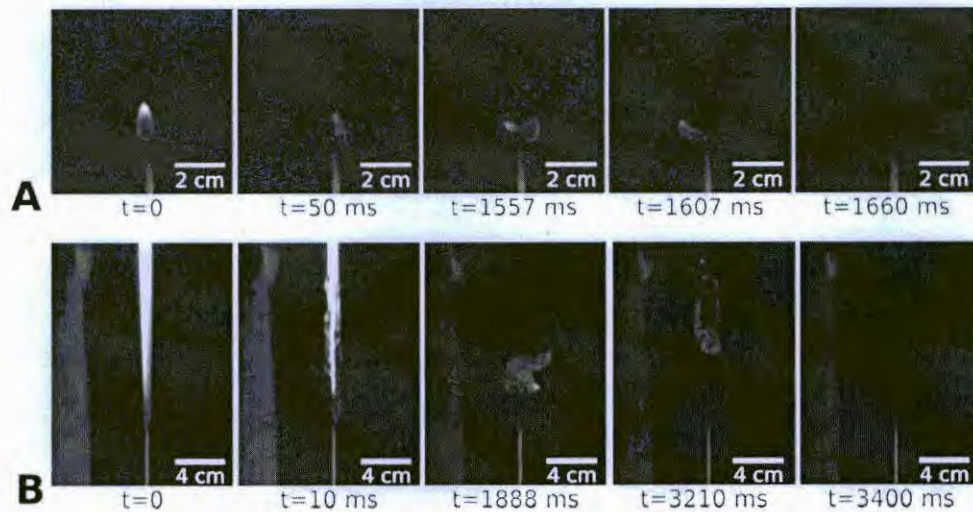


Figure 16. Hi-speed images of acoustic extinction at 75 Hz for methane flame from burner with ID = 0.0625". (A) Fuel velocity at the exit of the burner was 0.6 m/s. Extinction occurred after approximately 1.7 s. (B) Fuel velocity at exit of the burner was 20 m/s.

The mechanisms for oscillating streams of air interacting with the flame are similar to those we have observed under acoustic excitation³². With the application of oscillating air currents at low velocities, deformation of the flame body occurs and combustion rate is enhanced as fuel and oxygen are supplied to the combustion region. However, as the air velocity is increased additional phenomena occurred in the flame including (a) a decrease in the thickness of the flame boundary, (b) changes in the gradient between fuel and oxygen, (c) increases in the reactant concentration and production, (d) a decrease in the mean temperature of the flame. We have observed each of these occurrences throughout several experiments in Phase II.

At the NRL CBD, we observed vitiation and blow-off occurring with a liquid heptane flame. The flame area widened and began to lift away from the surface of the burner to regions where fuel/oxidizer ratio was sufficient to maintain combustion at a distance of approximately 6cm above the liquid pool. This observation supports the hypothesis that a change in the gradient between the fuel and oxidizer of the flame occurs under applied acoustic excitation. Additionally, we introduced thermocouple probes into flames and observed a rapid decrease in temperature upon acoustic interactions, even though we were unable resolve temperature changes on the same time scale of the applied acoustic frequency (the sampling rate of the probes was ~10 Hz).

5. Scale-up: Limitations and Opportunities

5.1. Limitations. Large scale extinction will be difficult using the existing schemes for extinction. From acoustic mapping of the speaker, we observe that the air velocity decreases rapidly from the collimator (**Figure 17**). Sound attenuation from most acoustic sources leads to a decrease in the acoustic power, and thus air velocity, at a large distance from the acoustic source. The magnitude of air velocities at a large distance from the speaker can be increased with the power of the speaker but will generally emanate in a conical geometry radiating from the speaker or collimator. You can see the effect of distance on the acoustic output in **Figure 2**, where we see a decrease in the measured sound pressure levels with distance from the speaker.

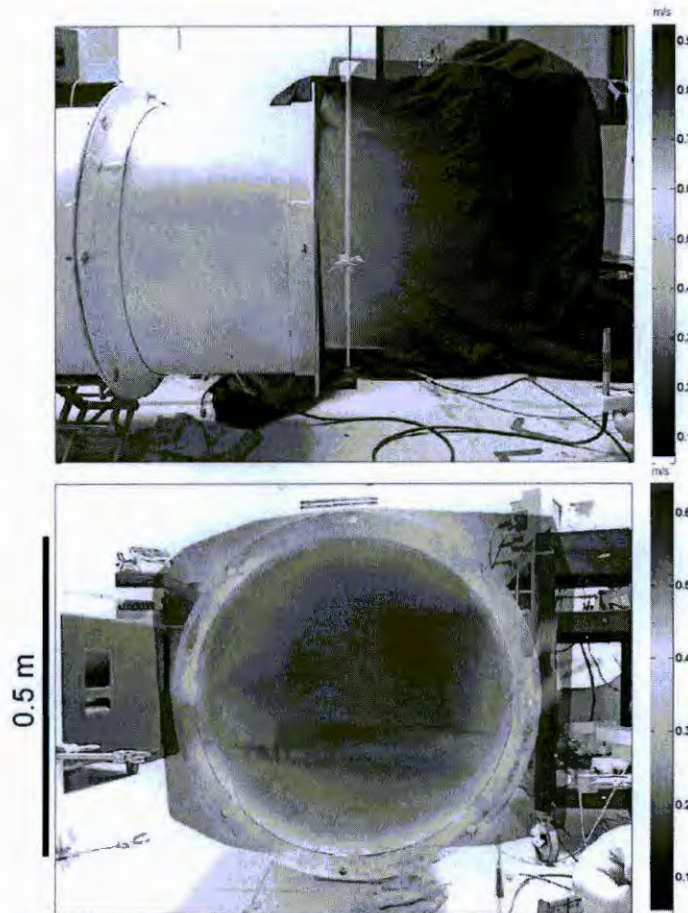


Figure 17. Acoustic velocity profile from collimated speaker measured using Microflow™ imaging systems.

In order to extinguish large area flames acoustically using the current setup, either a larger or more powerful (higher SPL output) speaker would need to be used. Directly increasing the output power of a speaker, will cause signal clipping; a distortion of the output signal. When dealing with a clipped system, the output will often be irregular and non-sinusoidal. One can multiplex speakers to achieve extinction of larger flames, however the practicality of such a system comes into question. To achieve extinction of a large area flame, several speakers can be placed in series so that their acoustic profiles overlap to affect a larger area. To achieve greater pressures in the system, you can align speakers so that their collimators face each other. Note

that in this orientation the phase of the applied acoustic signals must be monitored so they do not cancel each other out at the flame. All flames measured in this phase were smaller than the diameter of the collimator. Lastly, one could incorporate a technique of acoustic suppression using the phenomena described with acoustic cavities (Section 3). With knowledge of the resonant behavior of a room or enclosure, you could incorporate a single (or multiple) speaker within it to achieve acoustic velocities in specific areas of interest. This technique of suppression would require knowledge of the geometry of the acoustic cavity, so that the optimum placement of the speaker(s) can be achieved, as well as excitation with optimal the resonant frequencies for the room.

5.2. Opportunities. During the scale up efforts in Phase II, we found several phenomena that can be exploited for extinction and enhancement of the flame. By compiling extinction data collected from various fuels, we observed a trend in the extinction profiles. The acoustic pressures necessary for extinction were highly dependent on the fuel source but not the area of the flame. **Figure 18** displays the acoustic pressure necessary for the extinction of methane, ethanol, hexane, and heptanes fuels of differing burner areas.

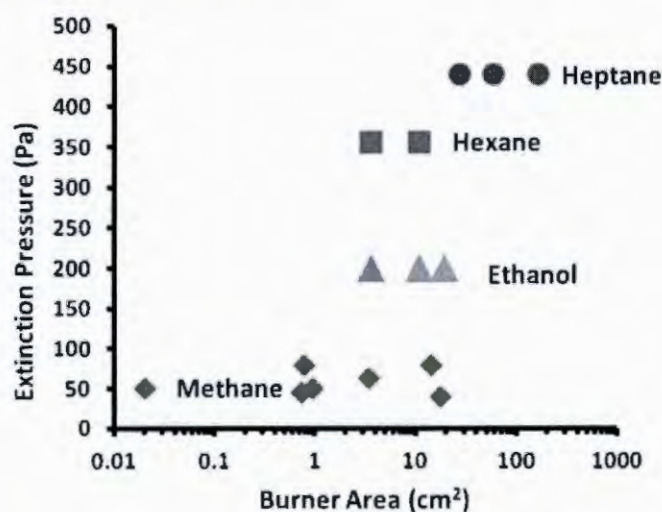


Figure 18. Acoustic extinction pressure of flames from multiple fuel sources against the total burner area of the fuel.

We also measured the fuel consumption rate of a liquid flame (hexane) during acoustic excitation (**Figure 19**). A known mass of fuel was loaded into a commercial wickless burner. Once ignited, the flame was exposed to acoustic excitations for 30 seconds and followed immediately by measuring the remaining mass of the fuel. The increased rate of fuel consumption was most likely due to increased mixing within an acoustic field. We conducted a similar study with solid fuels. We ignited a coal and exposed it to an acoustic field. The average heat of the coal surface increased from 460 to 530°C, as measured from an IR camera. This opens up a possible application of acoustics to improve combustion systems.

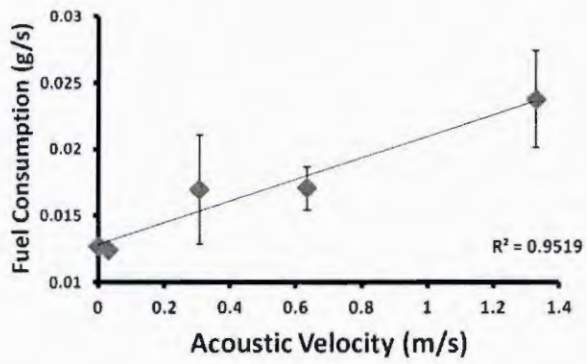


Figure 19. Fuel consumption of a hexane flame during acoustic excitation. The flame was exposed to an acoustic signal of 50Hz, at varying amplitudes to produce the measured velocities.

6. References

- (1) Candel, S. *Proceedings of the Combustion Institute* **2002**, 29, 1.
- (2) Poinso, T.; Yip, B.; Veynante, D.; Trounev, A.; Samaniego, J. M.; Candel, S. *Journal De Physique Iii* **1992**, 2, 1331.
- (3) Ziada, S.; Graf, H. *Journal of Fluids and Structures* **1998**, 12, 491.
- (4) Roh, T. S.; Tseng, I. S.; Yang, V. *Journal of Propulsion and Power* **1995**, 11, 640.
- (5) Sohn, C. H.; Chung, S. H.; Kim, J. S.; Williams, F. A. *Aiaa Journal* **1996**, 34, 1847.
- (6) Dowling, A. P.; Stow, S. R. *Journal of Propulsion and Power* **2003**, 19, 751.
- (7) Hauser, M.; Lorenz, M.; Sattelmayer, T. *Journal of Engineering for Gas Turbines and Power-Transactions of the Asme* **2011**, 133.
- (8) Lawn, C. J.; Evesque, S.; Polifke, W. *Combustion Science and Technology* **2004**, 176, 1331.
- (9) Marston, P. L.; Thiessen, D. B. In *Transport Phenomena in Microgravity 2004*; Vol. 1027, p 414.
- (10) Davis, M. R.; Lin, L. H. *Combustion and Flame* **1995**, 103, 151.
- (11) Demare, D.; Baillot, F. *Combustion and Flame* **2004**, 139, 312.
- (12) Plaks, D.; Nelson, E.; Hyatt, N.; Espinosa, J.; Coley, Z.; Tran, C.; Mayo, B. d. *The Journal of the Acoustical Society of America* **2005**, 118, 1945.
- (13) Kim, J. S.; Williams, F. A. *Combustion and Flame* **1994**, 98, 279.
- (14) Fachini, F. *Combustion Science and Technology* **1996**, 120, 237.
- (15) McKinney, D. J.; Dunn-Rankin, D. *Combustion Science and Technology* **2000**, 161, 27.
- (16) Sohn, C. H.; Chung, S. H. *Combustion and Flame* **2000**, 121, 288.
- (17) Komiyama, M.; Kawabe, R.; Takagi, T. *Proceedings of the Combustion Institute* **2009**, 32, 1099.
- (18) Kim, K. T.; Lee, J. G.; Quay, B. D.; Santavicca, D. A. *Combustion and Flame* **2010**, 157, 1731.
- (19) Babcock, W. R.; Baker, K. L.; Cattaneo, A. G. *Nature* **1967**, 216, 676.
- (20) Kim, N. I.; Lee, U. D.; Shin, H. D. *Combustion and Flame* **2004**, 136, 467.
- (21) Okai, K.; Moriue, O.; Araki, M.; Tsue, M.; Kono, M.; Sato, J.; Dietrich, D. L.; Williams, F. A. *Proceedings of the Combustion Institute* **2000**, 28, 977.
- (22) McIntosh, A. C. *Combustion Science and Technology* **1986**, 49, 143.
- (23) Pun, W.; Palm, S. L.; Culick, F. E. C. *Combustion Science and Technology* **2003**, 175, 499.
- (24) Buckmaster, J.; Clavin, P.; Linan, A.; Matalon, M.; Peters, N.; Sivashinsky, G.; Williams, F. A. *Proceedings of the Combustion Institute* **2005**, 30, 1.
- (25) Clavin, P.; Sun, J. *Combustion Science and Technology* **1991**, 78, 265.
- (26) Durox, D.; Schuller, T.; Candel, S. *Proceedings of the Combustion Institute* **2002**, 29, 69.
- (27) Pelce, P.; Rochwerger, D. *Journal of Fluid Mechanics* **1992**, 239, 293.
- (28) Putnam, A. A. *Science* **1953**, 117, 3.
- (29) Searby, G.; Rochwerger, D. *Journal of Fluid Mechanics* **1991**, 231, 529.
- (30) Clavin, P.; Pelce, P.; He, L. T. *Journal of Fluid Mechanics* **1990**, 216, 299.
- (31) Ledder, G.; Kapila, A. K. *Combustion Science and Technology* **1991**, 76, 21.
- (32) Kanury, A. M. *Introduction to combustion phenomena : (for fire, incineration, pollution, and energy applications)*; Gordon and Breach: New York, 1975.

Appendix 1. P-P Method (initially developed with Kyle Bishop)

Start with the following acoustic relation...

$$\frac{\partial \mathbf{v}}{\partial t} + \frac{1}{\rho_0} \nabla p = 0 \quad (\text{see Landau Lifshitz, Fluid Mechanics, p. 251})$$

Here, \mathbf{v} is the fluid velocity, ρ_0 is the fluid density, and p is the pressure variation about atmospheric pressure, p_0 . This equation comes from Euler's equation, which describes inviscid flow in a compressible fluid:

$$\frac{\partial \mathbf{v}}{\partial t} + \mathbf{v} \cdot \nabla \mathbf{v} = -\frac{\nabla p}{\rho}$$

Lifshitz states that because the oscillatory rarefactions and compressions of a sound wave are small, the term $\mathbf{v} \cdot \nabla \mathbf{v}$ is small or negligible. When \mathbf{v} and p vary sinusoidally with a single frequency (as is the case in our experiments), one can rewrite the equation above to give

$$\hat{\mathbf{v}} = \frac{i}{\omega \rho_0} \nabla \hat{p} \quad \text{with } \mathbf{v} = \text{Re}[\hat{\mathbf{v}} \exp(i\omega t)] \text{ and } p = \text{Re}[\hat{p} \exp(i\omega t)]$$

Just to break down Kyle's math on the substitution of the complex expressions into the first equation, we have the following:

$$\begin{aligned} i\omega \hat{\mathbf{v}} e^{i\omega t} + \frac{1}{\rho_0} \nabla \hat{p} e^{i\omega t} &= 0 \\ i\omega \hat{\mathbf{v}} + \frac{1}{\rho_0} \nabla \hat{p} &= 0 \\ \hat{\mathbf{v}} &= -\frac{1}{i\omega \rho_0} \nabla \hat{p} \end{aligned}$$

Thus, the velocity can be inferred from spatial gradients in the complex pressure coefficient. Here, we approximate the pressure gradient in a single direction (let's call it the x -direction) as

$$\hat{v}_x = \frac{i}{\omega \rho_0} \left(\frac{\hat{p}(x + \Delta x) - \hat{p}(x)}{\Delta x} \right)$$

Importantly, we *assume* that the pressure varies linearly over distances of Δx , and we calculate the complex coefficients for the pressure of the "Closer" microphone and the "Farther" microphone.

$$\hat{p}(\text{Closer}) = \text{Closer}(j).\text{real} + i\text{Closer}(j).\text{imag}$$

$$\hat{p}(\text{Farther}) = \text{Farther}(j).\text{real} + i\text{Farther}(j).\text{imag}$$

The velocity coefficient is then calculated as

$$\hat{v}_x = \frac{i}{\omega \rho_0 \Delta x} (\hat{p}(\text{Farther}) - \hat{p}(\text{Closer}))$$

Without using complex math and referring to p.91 of Fahy's *Sound Intensity*, we have the following:

$$\frac{\partial p}{\partial n} = -\rho_0 \frac{\partial u_n}{\partial t}$$

which is the same equation from Lifshitz. The parameter n corresponds to the direction of interest and u_n is the velocity in the specified direction. Fahy states the following using the above equation:

$$u_n(t) = -1/(\rho_o \Delta x) \int_{-\infty}^t \frac{\partial p(\tau)}{\partial n} d\tau$$

and then provides the following finite-difference approximation:

$$u_n(t) \approx 1/(\rho_o \Delta x) \int_{-\infty}^t [p_1(\tau) - p_2(\tau)] d\tau$$

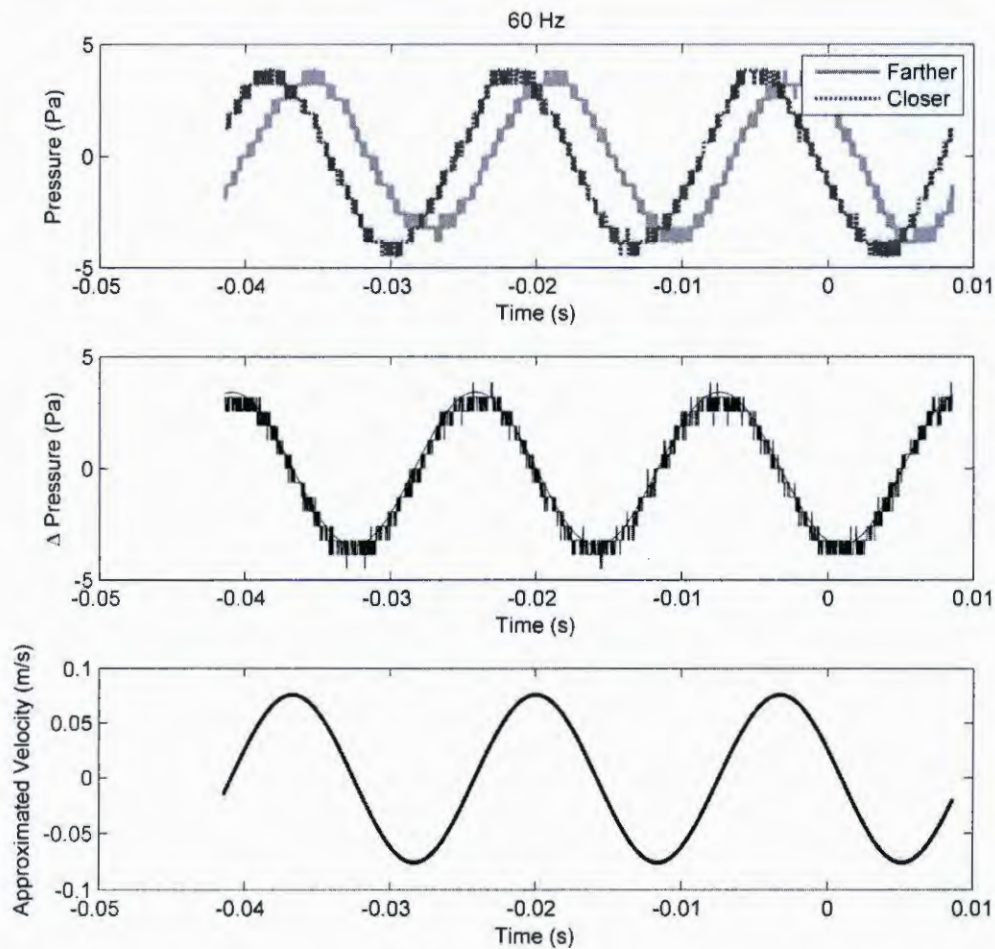
Using the data we collected, we can take the difference of the two pressure sine waves and then fit a curve of the following form to the oscillating differences in pressure:

$$p_1(\tau) - p_2(\tau) = P_{dif} \sin(\omega_{dif} t + \phi_{dif})$$

By performing integration on the above expression, we get an expression for the velocity:

$$u_n(t) \approx -P_{dif}/(\rho_o \Delta x \omega_{dif}) \cos(\omega_{dif} t + \phi_{dif})$$

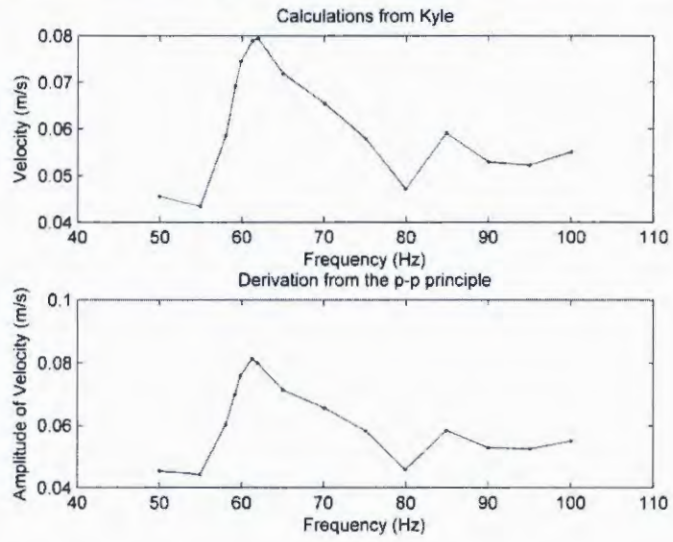
The following figure shows one example:



If we know the amplitude of the difference of the pressure, the amplitude of the velocity is given by

$$|u_n| \approx P_{dif} / (\rho_o \Delta x \omega_{dif})$$

The differences between this result and Kyle's result are negligible as shown below.



Appendix 2. Total Air Displacement from Measured Velocities

Given an oscillating velocity in time, we have the following:

$$v = v_o \sin(\omega t)$$

Using the P-P method or the Microflown, we would measure:

$$v_{rms} = \frac{v_o}{\sqrt{2}}$$

Now, to go from velocity to displacement, we can integrate the first expression:

$$\begin{aligned} d &= \int v dt \\ &= \frac{-v_o}{\omega} \cos(\omega t) \end{aligned}$$

The total displacement that we report is twice the amplitude (peak-peak displacement) and has the following form:

$$\begin{aligned} d_{total} &= 2 \left| \frac{-v_o}{\omega} \right| \\ &= \frac{2v_o}{\omega} \end{aligned}$$